Tunnelling and impact ionization in scaled double doped PHEMTs

K. Kalna and A. Asenov
Device Modelling Group, Dept. of Electronics & Electrical Engineering
University of Glasgow, Glasgow G12 8LT
Scotland, United Kingdom
E-mail:kalna@elec.gla.ac.uk

Abstract

We investigate the dominant breakdown mechanism in aggressively scaled pseudomorphic high electron mobility transistors (PHEMTs) with double delta-doping structure by Monte Carlo device simulations. Two breakdown mechanisms: channel impact ionization and thermionic tunnelling from the gate, are considered for two possible placements of the second delta doping layer either below the channel or between the gate and the first delta doping layer. Thermionic tunnelling starts at very low drain voltages but quickly saturates having a greater effect on those PHEMTs with the second doping layer placed above the original doping. A threshold for impact ionization occurs at larger drain voltages which should assure the reasonable operation voltage scale of double doped PHEMTs. Those double doped PHEMTs with the second delta doping layer placed below the channel deteriorate faster with the reduction of the channel length due to impact ionization than those devices with the second doping layer above the original doping.

1. Introduction

Both DC and RF performances of pseudomorphic high electron mobility transistors (PHEMTs) can be steadily improved when these devices are scaled into deep sub-100 nm dimensions [2]. To benefit from the improvement a full scaling approach has to be employed in which the devices are scaled down in both lateral and vertical dimensions in respect to gate lengths of $120, 70, 50$, and 30 nm [1]. If the scaling is applied only in lateral PHEMT dimensions then the performance of the sub-100 nm gate length devices deteriorates [**?**, 1, 3]. However, the carrier density in the channel drops because of reduction of the gate-to-channel distance in the proportional scaling process. The reduction in the carrier density, which affects the power handling capability of the devices, may be compensated when an additional delta doping layer is placed into the PHEMT structure [5] in order to increase the drive current. If a second delta doping layer is placed below the channel [see Fig. 1(a)], the transconductance peak broadens resulting in large improvement in the device linearity, although the maximum transconductances remain close to the corresponding values in single delta doped devices [6].

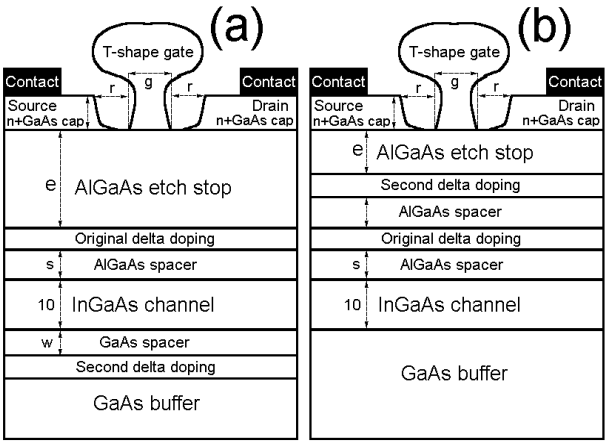

Figure 1. Cross sections of PHEMT with two positions of the additional doping: (a) the second delta doping layer below the channel or (b) the second delta doping above the original doping layer.

If the second delta doping layer is placed above the original delta doping, near to the gate, the maximum transconductance increases by up to 80% for the 70 nm device as shown in Fig. 2. This effect is however reduced with the PHEMT scaled to 50 nm and below [6].

The reduction of the gate to channel separation in the proportional scaling increases the probability for electron tunnelling from the gate, which may trigger breakdown. Also because the carrier density in the channel substantially increases with additional delta doping the device becomes more sensitive to channel impact ionisation. In this work we have investigated two concurrent breakdown mechanisms: channel impact ionization which first occurs around the gate corner on the drain side of the channel due to a fringing electric field [7] (see Fig. 4) and gate tunnelling which causes gate current leakage and may itself trigger avalanche breakdown [8] (see Fig 1).

2. Impact ionization and tunnelling

This study has been carried out with our finite element Monte Carlo (MC) device simulator MC/H2F. The MC/H2F employs quadrilateral finite elements to depict the complex geometry around the T-shape gate and recesses of the PHEMT. The MC module contains electron

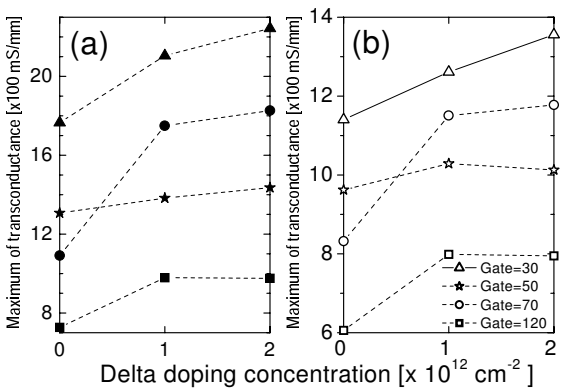

Figure 2. Maximum of transconductance as a function of the doping concentration in the second doping layer placed above the original doping for an intrinsic device (a) and with external resistances included (b).

scattering with polar optical phonons, inter- and intra-valley optical phonons, non-polar optical phonons and acoustic phonons, as well as ionized and neutral impurity scattering. The alloy potential scattering and strain effects on bandgaps, electron effective masses, phonon deformation potentials and energies are taken into account in the InGaAs channel. All scattering rates consider a form factor F (the overlap integral) given by

$$F(E,E') = \frac{(1+\alpha E)(1+\alpha' E') + \frac{1}{3}\alpha E\,\alpha' E'}{(1+2\alpha E)(1+2\alpha' E')}, \quad (1)$$

where an electron with the initial energy E has the final energy E' after a scattering. α and α' in the relation (1) are the non-parabolicity parameters for the electron in initial and final valleys respectively.

Impact ionization is included in the device simulator MC/H2F as an additional scattering mechanism. If impact ionization starts at a threshold energy $E_{\rm th}$ then the electron scattering rate reads [9]

$$\Gamma(E) = P\,[(E-E_{\rm th})/E_{\rm th}]^A, \quad (2)$$

where P and A are parameters which must be fitted to experimental data. Note here that the formula (2) is nothing more than a fitting expression based on Keldysh model for impact ionization. Such fitting expressions are often used in MC device simulations [10] due to the complexity of quantum mechanical approaches. We have used $A = 4$ for GaAs as it has been suggested in Ref. 9 and $A = 14$ for $In_{0.53}Ga_{0.47}As$ which is more difficult to simulate at a very high electric field. Bulk simulations of the impact ionization coefficient can satisfactorily reproduce measured data for GaAs and $In_{0.53}Ga_{0.47}As$ in the range of electric fields of interest [11]. Since hole dynamics and the corresponding bipolar effects are not included in the H2F/MC, the experimentally observed increase in the drain current at breakdown cannot be reproduced. Instead, we calculate an impact ionization assisted increase in the electron current of the devices. This allows us to define the bias conditions

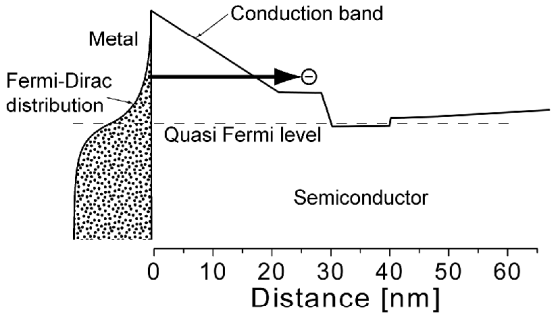

Figure 3. Cross section of the device through the middle of the gate at gate and drain biases of -1.0 and 2.0 V respectively. The tunnelling from the gate into the device is schematically shown.

corresponding to the onset of impact ionization which is determined only by the electron dynamics.

Thermionic tunnelling is incorporated into the MC/H2F as an additional simulation procedure during each time step and proceeds as follows: a number of particles (which represent the electron density in the metal) is obtained after integration over the Fermi-Dirac distribution. Fig. 3 schematically illustrates the area of the Fermi-Dirac distribution from which the particle of a randomly selected energy E may tunnel into the device. In this way, the thermal broadening of electron distribution at room temperature is included into the tunnelling model. The tunnelling probability, T, is numerically calculated from the WKB approximation [12] by evaluating the integral

$$T(E) = \exp\{-2\frac{\sqrt{2m}}{\hbar}\int_0^w [V(x)-E]^{1/2}\,dx\}, \quad (3)$$

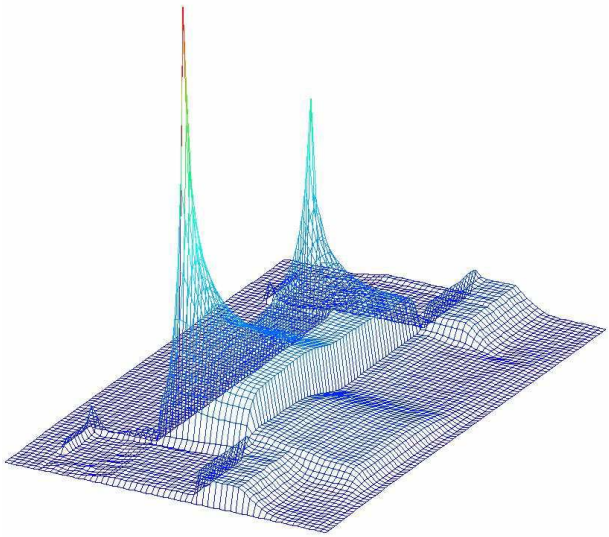

Figure 4. Electric fields in the 120 nm PHEMT at $V_G = -1.0$ V and $V_D = 2.0$ V. The huge electric field surrounds the gate and peaks beneath the gate corners.

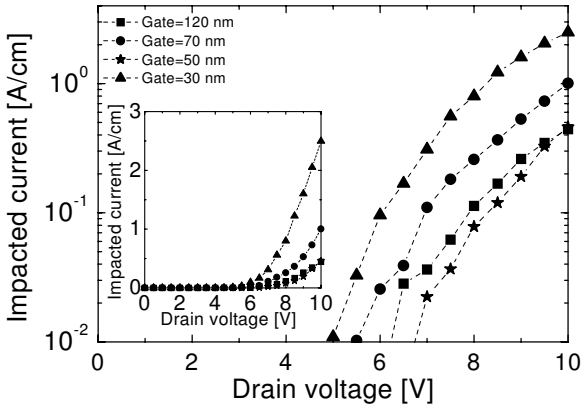

Figure 5. Impact ionization assisted drain current versus the drain voltage at V_G=−1.0 V for double doped scaled PHEMTs with the second delta doping layer above the original doping.

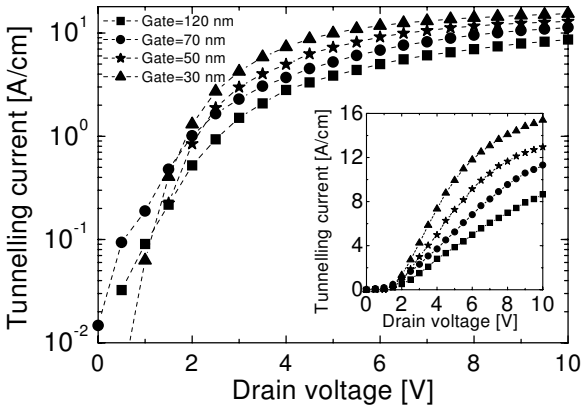

Figure 6. Thermionic tunnelling assisted gate current versus the drain voltage at V_G=−1.0 V for double doped scaled PHEMTs with the second delta doping layer above the original doping, near to the gate.

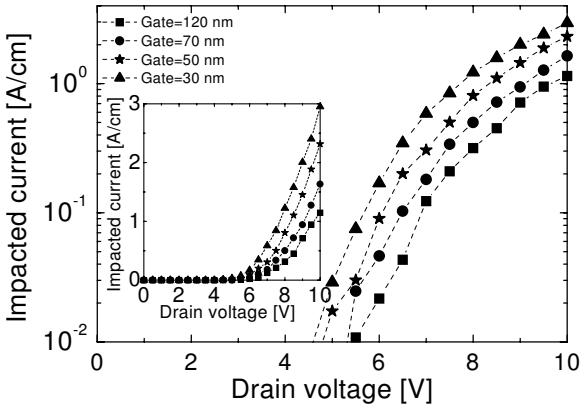

Figure 7. Impact ionization assisted drain current versus the drain voltage at V_G=−1.0 V for double doped scaled PHEMTs with the second delta doping layer below the channel.

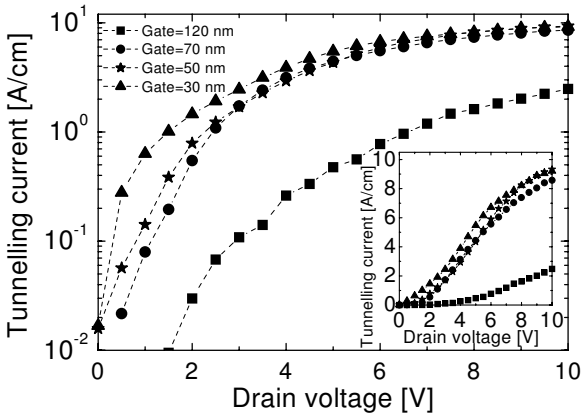

Figure 8. Thermionic tunnelling assisted gate current versus the drain voltage at V_G=−1.0 V for double doped scaled PHEMTs with the second delta doping layer below the channel.

where m is the electron effective mass in the device, w is the path along which the electron should tunnel through and $V(x)$ is the potential. This probability is used in a standard rejection technique to accept or reject the tunnelling event. If the tunnelling is accepted then the particle will be injected into the device at the energy E. The particle is injected in the direction of the strongest electric field (see Fig. 4). This process is repeated for each particle and at each mesh cell around the gate. The number of tunnelling particles is then used to calculate the gate tunnelling current.

3. Assisted drain currents

The layout of a typical PHEMT under investigation is shown in Fig. 1(a). It has a T-shape gate; a 30 nm heavily doped (4×10^{18}cm^{-3}) n+ GaAs cap; an $Al_{0.3}Ga_{0.7}As$ etchstop; a 7×10^{12}cm^{-2} Si delta doping; an $Al_{0.3}Ga_{0.7}As$ spacer; a 10 nm $In_{0.2}Ga_{0.8}As$ channel; a second $Al_{0.3}Ga_{0.7}As$ spacer and a second 4×10^{12}cm^{-2} Si delta doping. The whole device structure is grown on top of a 50 nm thick GaAs buffer. The MC device simulator itself has been accurately calibrated (by calculating I_D-V_D characteristics for several fixed gate voltages) against a real single doped 120 nm PHEMT fabricated at the University of Glasgow [1]. Note that the inclusion of external resistances is required to compare the simulated I_D-V_D characteristics obtained directly from the MC/H2F with experimental data.

The corresponding threshold drain voltage for both breakdown mechanisms, impact ionization and thermionic tunnelling, is calculated from a number, N, of impacted or, respectively, tunnelled particles during the simulation time, t, as

$$I_D^{\text{assist}} = N\frac{e_S}{t}, \tag{4}$$

where e_S is the charge of superparticle. These assisted drain currents are examined in double doped scaled PHEMTs with the two possible placement of the second delta doping layer. Figs. 5 and 7 show the impact ionization assisted drain current as a function of the applied drain voltage at a very low gate bias of -1.0 V. Impact ionization quickly starts to increase the drain current which could finally lead to complete device breakdown. Figs. 6 and 8 show the thermionic tunnelling assisted gate current again as a function of the drain voltage at the same gate bias. It is clear that the current due to thermionic tunnelling has a different drain voltage dependence compared to the impact ionisation current; increasing relatively sharply at lower drain voltages [13] but then saturates at larger drain voltages. The thresholds for both impact ionization and thermionic tunnelling decrease with device scaling. The threshold for the impact ionization assisted drain current in Fig. 5 (for double doped PHEMTs with the second delta doping above the original doping) starts at slightly lower drain voltages compared to the single doped devices [11]. This is due to the fact that the second delta doping screens the penetration of the gate fringing field in the channel at the drain corner. This is also supported by the fact that the threshold for the impact ionization assisted drain current in Fig. 7 (for double doped PHEMTs with the second delta doping below the channel) is larger then those in Fig. 5. Figs. 6 and 8 show that although the thermionic tunnelling assisted gate current starts at a very low drain voltage, rapidly saturating at large drain voltages even for devices with very small gate-to-channel separation. Therefore it should not be of great concern for the scaling process. The placement of the second delta doping layer near to the gate (Fig. 6) produced more thermionic tunnelling assisted gate current compared to the design with the second delta doping layer below the channel (Fig. 8). The gate tunnelling current in Fig. 6 also steadily increases with the scaling while the current in Fig. 8 remains practically constant in 70, 50 and 30 nm double doped PHEMTs with the second delta doping layer below the channel.

4. Conclusion

Using MC device simulations we have evaluated two breakdown mechanisms, channel impact ionization and gate thermionic tunnelling, which are responsible for device breakdown. Two possible placements of the second delta doping layer in the double doped PHEMTs have been considered following our previous work on PHEMT scaling [6]. When the second delta doping layer is placed above the original delta doping, near to the gate, the device exhibits an improvement in the transconductance compared to the respective single doped PHEMTs. Nevertheless, this type of the design has larger leakage due to gate tunnelling. The effect of impact ionization is slightly smaller than in the other double doped design. When the second delta doping layer is placed below the channel the device transconductance slightly deteriorates but the device linearity substantially improves [6]. This placement of second delta doping does not affect the thermionic tunnelling assisted gate current which remains practically the same as in the single doped PHEMTs. This type of design causes a small increase in the impact ionization assisted drain current due to a higher electric fringing field compared to the former design. However, impact ionization itself always increases so dramatically that the crucial task in PHEMT design is to make the impact ionization threshold as high as possible.

Acknowledgement. This work has been supported by EPSRC under Grant No. GR/M93383.

[1] K. Kalna, S. Roy, A. Asenov, K. Elgaid, and I. Thayne, "Scaling of pseudomorphic high electron mobility transistors to decanano dimensions", *Solid-State Electron.* **46** (2002) 631-638.

[2] K. Kalna, S. Roy, A. Asenov, K. Elgaid, and I. Thayne, "RF analysis of aggressively scaled pHEMTs", in *Proceedings of ESSDERC 2000*, ed. by W. A. Lane, G. M. Crean, F. A. McCabe and H. Grünbacher (2000) 156-159.

[3] I. C. Kizilyalli, K. Hess, J. L. Larson, and J. D. Widinger, "Scaling properties of high electron mobility transistors", *IEEE Trans Electron Devices* **33** (1986) 1427-1433.

[4] M. B. Patil, U. Ravaioli, and M. R. Hueschent, "Monte Carlo simulation of real-space transfer transistors: Device physics and scaling effects" *IEEE Trans Electron Devices* **40** (1993) 480-486.

[5] K. W. Lin, K. H. Yu, W. L. Chang, C. C. Cheng, K. P. Lin, C. H. Yen, W. S. Lour, and W. C. Liu, "Characteristics and comparison of $In_{0.49}Ga_{0.51}P$/InGaAs single and double delta-doped pseudomorphic high electron mobility transistors", *Solid-State Electron.* **45** (2001) 309-314.

[6] K. Kalna and A. Asenov, "Multiple delta doping in aggressively scaled PHEMTs", in *Proceedings of ESSDERC 2001*, ed. by H. Ryssel, G. Wachutka, and H. Grünbacher (2001) 380-384.

[7] J. Han and D. K. Ferry, "Scaling of gate length in ultra-short channel heterostructure field effect transistors," *Solid-State Electron.* **43** (1999) 335-341.

[8] J. S. Kleine, Q. D. Qian, J. A. Cooper, and M. R. Melloch, "Electron emission from direct bandgap heterojunction capacitors", *IEEE Trans. Electron Devices* **36** (1989) 289-299.

[9] M. Stobbe, R. Redmer, and W. Schattke, "Impact ionization rate in GaAs" *Phys. Rev.* B **49** (1994) 4494-4500.

[10] C. J. Wordelman, "3-D granular Monte Carlo simulations of semiconductor devices", PhD thesis, Urbana, Illinois (2000) p 13.

[11] K. Kalna, A. Asenov, K. Elgaid, and I. Thayne, "Effect of Impact Ionization in scaled pHEMTs", *Proceedings of EDMO2000*, IEEE publication, Glasgow (2000) 236-241.

[12] D. K. Roy, "Quantum mechanical tunnelling and its applications", World Scientific, New York (1986) p 17.

[13] M. H. Somerville, C. S. Putnam, and J. A. del Alamo, "Determining dominant breakdown mechanism in InP HEMTs", *IEEE Electron Device Lett.* **22** (2001) 565-567.